

Semiclassical Catastrophe Theory of Simple Bifurcations

A. G. Magner*

Institute for Nuclear Research, 03680 Kyiv, Ukraine

K. Arita

Department of Physics, Nagoya Institute of Technology, Nagoya 466-8555, Japan

(Dated: November 19, 2019)

The Fedoriuk-Maslov catastrophe theory of caustics and turning points is extended for solving the bifurcation problems by the improved stationary phase method (ISPM). The trace formulas for the radial power-law (RPL) potentials are presented by the ISPM based on the second- and third-order expansion of the classical action near the stationary point. A considerable enhancement of contributions of the two orbits (pair of the parent and newborn ones) at their bifurcation is shown. The ISPM trace formula is proposed for a simple bifurcation scenario of Hamiltonian systems with continuous symmetries, where the contributions of the bifurcating parent orbits vanish as approaching the bifurcation point due to the reduction of the end-point manifold. This occurs since the contribution of the parent orbits is included into the term corresponding to the family of the new-born daughter orbits. Taking this feature into account, the ISPM level densities calculated for the RPL potential model are shown to be in good agreement with the quantum results at the bifurcations and asymptotically far from the bifurcation points.

I. INTRODUCTION

Semiclassical periodic-orbit theory (POT) is a powerful tool for the study of shell structures in the single-particle level density of finite fermionic systems [1–4]. This theory relates the oscillating level density and shell-correction energy to the sum over contributions of the classical periodic orbits. It thus gives the correspondence between the fluctuation properties of the quantum dynamics and the characteristics of the periodic motion embedded in the classical dynamics.

Gutzwiller [2] suggested the semiclassical evaluation of the Green's function in the Feynman path integral representation to derive the POT trace formula for the level density if the single-particle Hamiltonian has no continuous symmetries other than the time-translational invariance. In this case, the energy E is the single integral of motion for a particle dynamics in the mean-field potential. For a given E , all the generic periodic orbits (POs) are isolated, i.e., any variation of the initial condition perpendicular to the PO will violate its periodicity. The original version of the POT was extended for the Hamiltonians with continuous symmetries (extended Gutzwiller approach), in particular for the rotational ($O(n)$) and oscillator-type ($SU(n)$) symmetries [5–8]. Berry and Tabor [9] derived the POT for integrable (multiply-periodic) systems by applying the Poisson-summation method through the semiclassical torus-quantization condition. It is also helpful in the case of a high classical degeneracy of POs. Here, the classical degeneracy is defined by the number of independent parameters \mathcal{K} for a continuous family of the classical periodic orbits at a given energy of the particle.

Some applications of the POT to the deformations of nuclei and metallic clusters by using the phase-space variables were presented in Refs. [4, 6, 8–11]. The pronounced shell effects caused by the deformations have been discussed. Within the improved stationary-phase method [10–16] (improved SPM, or ISPM), the divergences and discontinuities of the standard SPM (SSPM) [3–5, 8, 9] near the symmetry-breaking and bifurcation points were removed.

Bifurcations of the isolated POs in non-integrable Hamiltonian systems are classified by the normal-form theory [17, 18], based on a pioneering work of Meyer on the differentiable symplectic mappings [19]. The change in the number of POs depends on the types of the bifurcations: From zero to two in the isochronous or “saddle-node” bifurcations, from one to three in the period-doubling or “pitchfork” bifurcations, and so on. In the integrable (multiply-periodic) systems, the classical phase space is entirely covered by the tori. The classical orbits on the rational tori (in which the frequencies of the independent motions are commensurable) form the degenerate families of POs. In such systems, the bifurcations mostly occur at a surface of the physical phase-space volume occupied by the classical trajectories. For shortness, such a surface will be called below the *end-points*. Note that even if the commensurability of the frequencies is not fully satisfied at the end point, one has a PO there because the mode with incommensurable frequencies has the zero amplitude. In the action-angle representation (I_n, Θ_n) for the n th mode, it corresponds to $I_n = 0$, where the variation of Θ_n will not generate a family. Thus, the end-point POs have smaller degeneracies than those inside the physical region. With varying the potential parameter, a new PO family appears in the transition from an unphysical to the physical region for a rational torus where the frequencies of the end-point PO become commensurable. It is considered as the bifurca-

* Email: magner@kinr.kiev.ua

tion of the end-point PO generating a new orbit family. Such bifurcations take place repeatedly with varying the potential parameter and a new family of orbit with a higher degeneracy and different frequency ratio is generated at each bifurcation point. Typical examples are the equatorial orbits with $\mathcal{K} = 1$ in the spheroidal cavity where the generic family has $\mathcal{K} = 2$, and the circular orbits with $\mathcal{K} = 2$ in a spherical potential where the generic family appears with $\mathcal{K} = 3$.

Our ISPM is based on the catastrophe theory by Fedoriuk and Maslov for solving problems with the caustic and turning points in calculations of the integrals by using the saddle-point method [13, 20–22]. In the SSPM, the catastrophe integrals are evaluated by an expansion of the action integral in the exponent up to the second-order terms and amplitude up to the zeroth order ones near the stationary point, and the integration limits are extended to the infinite interval. The trace formula based on the SSPM encounters a divergence or discontinuity at the bifurcation point. Such catastrophe problems are due to the zeros (caustics) or infinities (turning points) of the second-order derivatives of the action integral in this expansion. Fedoriuk was the first one who proved [20, 22] the so-called Maslov theorem [21]: Each simple caustic or turning point (having a finite nonzero third-order derivative of the action integral) leads to a shift of the phase in exponent of the catastrophe integral by $-\pi/2$ along the classical trajectory. This provides the extension of the one-dimensional WKB formula to higher dimensions. Thus, in the asymptotic region far from the caustic and turning points, one can use the second order expansions of the action integral (and zeroth order ones of the amplitude) in the semiclassical Green's function taking into account the shift of the phase according to the Maslov theorem. However, a proper foundation for an extension of the Fedoriuk-Maslov catastrophe theory (FMCT) to the derivations of the trace formulas near the PO bifurcations, where one has to treat the semiclassical propagators near the catastrophe points, is still an open question.

Uniform approximations based on the normal-form theories give alternative ways of solving the bifurcation problems, see Refs. [4, 8, 18, 23–32]. The trace formula valid near the bifurcation points is derived by calculating the catastrophe integral in the *local* uniform approximations. It gives an indistinct combination of the contributions of bifurcating POs, and the asymptotic regions (where each of the PO has a separate contribution to the trace integral) are connected by a kind of the interpolation through the bifurcations in the *global* uniform approximations. The ISPM provides much simpler semiclassical formula in which one needs no artificial interpolation procedures over the bifurcations. Within the simplest ISPM, the contributions of the bifurcating orbits are given separately through the bifurcation, and they are basically independent on the type of the bifurcation. This allows to give analytic expressions for the Gaussian-averaged level densities and the energy shell corrections

[4, 5, 33, 34].

In the present work, we apply the FMCT for solving the bifurcation problems which arise at some parameters of the mean-field potential for the particle motion in the end-point phase space. For a simplest but a rich exemplary case which, nevertheless, includes all of necessary points of the general behavior of the integrable systems, we shall consider the spherical radial power-law (RPL) potential, $V \propto r^\alpha$, as a function of the radial power parameter α which controls the surface diffuseness of the system [28, 31, 35]. Some of these results are general for any integrable and non-integrable Hamiltonian systems, and can be applied to a more realistic nuclear mean-field potential having the deformation. The spherical RPL model has been already analyzed within the ISPM in Ref. [11]. A good agreement between the semiclassical and quantum shell structures was shown in the level-density and energy shell corrections for several values of the surface diffuseness parameter including its symmetry-breaking and bifurcation values. Quantum-classical correspondences in the deformed RPL models with and without spin-orbit coupling were also studied, and various properties of the nuclear shape dynamics, such as the origins of exotic deformations and the prolate-oblate asymmetries, have been clarified [11, 31, 35, 36, 38]. Therefore, a proper study of the general aspects of the bifurcation problem within the ISPM, even taking the simplest spherical RPL potential as an example for which one can achieve a far-going progress in analytical derivations, is expected to be helpful.

This article is organized in the following way. In Sec. II, we present a general semiclassical phase-space trace formula for the level density as a typical catastrophe integral. Section III shows the Fedoriuk-Maslov method for solving the simple caustic- and turning-point singularity problems. Section IV is devoted to the application of the FMCT to the local PO bifurcations for more general Hamiltonian systems with continuous symmetries. Section V presents the specific application of the ISPM trace formula to the bifurcations in the spherical RPL potential model. Contributions of the bifurcating orbits into the trace formula are discussed. In Sec. VI, we compare our semiclassical results, obtained at a bifurcation point and asymptotically far from bifurcations, with the quantum calculations. These results are summarized in Sec. VII. A more precised trace formula based on the third-order expansions of the action integral is presented in Appendix A.

II. TRACE FORMULA

The general semiclassical expression for the level density, $g(E) = \sum_i \delta(E - E_i)$, is determined by the energy levels E_i for the single-particle Hamiltonian $\hat{H} = \hat{T} + V$ of \mathcal{D} degrees of freedom. The specific expression generic to integrable and non-integrable systems can be obtained by

the following trace formula in the $2\mathcal{D}$ -dimensional phase space [11–15]:

$$g_{\text{scl}}(E) = \frac{1}{(2\pi\hbar)^{\mathcal{D}}} \text{Re} \sum_{\text{CT}} \int d\mathbf{r}' \int d\mathbf{p}' \delta(E - H(\mathbf{r}', \mathbf{p}')) \times |\mathcal{J}_{\text{CT}}(\mathbf{p}'_{\perp}, \mathbf{p}'_{\perp})|^{1/2} \exp\left(\frac{i}{\hbar} \Phi_{\text{CT}} - i\frac{\pi}{2} \mu_{\text{CT}} - i\phi_{\mathcal{D}}\right). \quad (1)$$

Here, $H(\mathbf{r}, \mathbf{p})$ is the classical Hamiltonian in the phase space variables \mathbf{r}, \mathbf{p} ; Φ_{CT} the phase integral,

$$\begin{aligned} \Phi_{\text{CT}} &\equiv [S_{\text{CT}}(\mathbf{p}', \mathbf{p}'', t_{\text{CT}}) + (\mathbf{p}'' - \mathbf{p}') \cdot \mathbf{r}''] \\ &= [S_{\text{CT}}(\mathbf{r}', \mathbf{r}'', E) + \mathbf{p}' \cdot (\mathbf{r}' - \mathbf{r}'')] , \end{aligned} \quad (2)$$

see the derivations in Ref. [11]. In Eq. (1), the sum is taken over all discrete classical trajectories (CT) for a particle motion from the initial point $(\mathbf{r}', \mathbf{p}')$ to the final point $(\mathbf{r}'', \mathbf{p}'')$ with a given energy E [13]. A CT can uniquely be specified by fixing, for instance, the final coordinate \mathbf{r}'' and the initial momentum \mathbf{p}' for a given time t_{CT} of the motion along a CT. $S_{\text{CT}}(\mathbf{p}', \mathbf{p}'', t_{\text{CT}})$ is the classical action in the momentum representation,

$$S_{\text{CT}}(\mathbf{p}', \mathbf{p}'', t_{\text{CT}}) = - \int_{\mathbf{p}'}^{\mathbf{p}''} d\mathbf{p} \cdot \mathbf{r}(\mathbf{p}). \quad (3)$$

The integration by parts relates Eq. (3) to the classical action in the coordinate space,

$$S_{\text{CT}}(\mathbf{r}', \mathbf{r}'', E) = \int_{\mathbf{r}'}^{\mathbf{r}''} d\mathbf{r} \cdot \mathbf{p}(\mathbf{r}), \quad (4)$$

by the Legendre transformation [Eq. (2)]. The factor μ_{CT} is the number of conjugate points along a CT with respect to the initial phase-space point $(\mathbf{r}', \mathbf{p}')$. They are, e.g., the focal and caustic points where the main curvatures of the energy surface (second derivatives of the phase integral Φ_{CT}) vanish. In addition, there are the turning points where these curvatures become divergent. The number of conjugate points evaluated along a PO is called the Maslov index [21]. An extra phase component $\phi_{\mathcal{D}}$, which is independent on the individual CT, is determined by the dimension of the system and the classical degeneracy \mathcal{K} ($\phi_{\mathcal{D}}$ is zero when all orbits are isolated ($\mathcal{K} = 0$), as defined in Ref. [2]).

In Eq. (1), we introduced the local phase-space variables which consist of the three-dimensional ($\mathcal{D} = 3$) coordinate, $\mathbf{r} = \{x, y, z\}$, and momentum, $\mathbf{p} = \{p_x, p_y, p_z\}$. It is determined locally along a reference CT so that the variables ($r_{\parallel} = x, p_{\parallel} = p_x$) are parallel and ($\mathbf{r}_{\perp} = \{y, z\}, \mathbf{p}_{\perp} = \{p_y, p_z\}$) are perpendicular to the CT [2, 4, 6]. $\mathcal{J}_{\text{CT}}(\mathbf{p}'_{\perp}, \mathbf{p}''_{\perp})$ is the Jacobian for the transformation of the momentum component perpendicular to a CT from the initial, \mathbf{p}'_{\perp} , to the final, \mathbf{p}''_{\perp} , values.

For calculations of the trace integral by the SPM, one may write the stationary phase conditions in both \mathbf{p}' and \mathbf{r}'' variables. According to the definitions (2) and (3), the stationary-phase conditions are given by

$$\begin{aligned} \left(\frac{\partial \Phi_{\text{CT}}}{\partial \mathbf{p}'}\right)^* &\equiv (\mathbf{r}' - \mathbf{r}'')^* = 0, \\ \left(\frac{\partial \Phi_{\text{CT}}}{\partial \mathbf{r}''}\right)^* &\equiv (\mathbf{p}'' - \mathbf{p}')^* = 0. \end{aligned} \quad (5)$$

The asterisk indicates that quantities in the circle brackets are taken at the stationary point. The above equations express that the *stationary-phase* conditions are equivalent to the *periodic-orbit* (PO) equations $(\mathbf{r}'', \mathbf{p}'')^* = (\mathbf{r}', \mathbf{p}')^*$. One of the SPM integrations in Eq. (1), e.g., over the parallel momentum p'_{\parallel} in the local Cartesian coordinate system introduced above, is the identity because of the energy conservation, $E = H(\mathbf{r}'', \mathbf{p}'') = H(\mathbf{r}', \mathbf{p}')$. Therefore, it can be taken exactly. If the system has continuous symmetries, the integrations with respect to the corresponding cyclic variables can be carried out exactly. Notice that the exact integration is performed finally also along a parallel spacial coordinate (along the PO).

Applying the ISPM with the PO equations (5), accounting for the bifurcations and the breaking of symmetries, one may arrive at the trace formula in terms of the sum over POs [4, 10, 11]. The total ISPM trace formula is the sum over all of POs [families with the classical degeneracy $\mathcal{K} \geq 1$ and isolated orbits ($\mathcal{K} = 0$)],

$$\delta g(E) \simeq \delta g_{\text{scl}}(E) = \sum_{\text{PO}} \delta g_{\text{PO}}(E), \quad (6)$$

where

$$\delta g_{\text{PO}}(E) = \text{Re} \left\{ A_{\text{PO}} \exp \left[\frac{i}{\hbar} S_{\text{PO}}(E) - \frac{i\pi}{2} \mu_{\text{PO}} - i\phi_{\mathcal{D}} \right] \right\}. \quad (7)$$

The amplitude A_{PO} depends on the classical degeneracy \mathcal{K} and the stability of the PO. $S_{\text{PO}}(E) = \oint \mathbf{p} \cdot d\mathbf{r}$ is the action, and μ_{PO} is the Maslov index [2, 4, 5, 10, 11].

III. FEDORIUK-MASLOV CATASTROPHE THEORY

In this section, we present the essence of the ISPM, following basically the Fedoriuk-Maslov catastrophe theory (see Refs. [20–22]).

A. Caustic and turning points

Let us assume that the integration interval in one of the integrals of Eq. (1) over a phase-space variable ξ contains a stationary catastrophe point where the second derivative of the phase integral Φ is zero [see Eq. (5)]. This catastrophe integral, $\mathcal{I}(\kappa, \epsilon)$, can be considered as a function of the two dimensionless parameters,

$$\mathcal{I}(\kappa, \epsilon) = \int_{\xi_-}^{\xi_+} d\xi A(\xi, \epsilon) \exp[i\kappa \Phi(\xi, \epsilon)], \quad (8)$$

where $A(\xi, \epsilon)$ is an amplitude and $\Phi(\xi, \epsilon)$ the dimensionless phase integral which is proportional to Φ_{CT} given by Eq. (1). One of these parameters, κ , is related to a large semiclassical parameter $\kappa \propto 1/\hbar \rightarrow \infty$, when $\hbar \rightarrow 0$, through the relationship $\kappa \Phi = \Phi_{\text{CT}}/\hbar$ (see also

Appendix A for a transparent example). Another critical parameter ϵ is a small dimensionless perturbation of the phase integral $\Phi(\xi, \epsilon)$ [Eq. (2)] and the amplitude $A(\xi, \epsilon)$ through the potential $V(\mathbf{r}, \epsilon)$. For instance, ϵ can be a dimensionless distance from the catastrophe point by perturbing the parameter of a potential $V(\mathbf{r}, \epsilon)$ [10], e.g., the deformation and diffuseness parameters (see examples in Refs. [4, 10, 11]). In Eq. (8), the integration limits ξ_{\pm} crossing the catastrophe point $\xi^*(0)$ are generally assumed to be *finite*.

We assume also that the integral (8) has the simplest (first-order) caustic-catastrophe point $\xi^*(\epsilon)$ at $\epsilon = 0$ defined by¹

$$\begin{aligned} \Phi'(\xi^*) &= 0, & \Phi''(\xi^*) &= 0, \\ \Phi'''(\xi^*) &= \mathcal{O}(\epsilon^0), & \text{at } \xi^* &= \xi_0 = \xi^*(0), \end{aligned} \quad (9)$$

where the asterisk indicates that the derivatives with respect to ξ are taken at $\xi = \xi^*$. The mixed derivative $(\partial^2 \Phi / \partial \xi \partial \epsilon)^*$, $A^* = A(\xi^*, \epsilon)$, is assumed to be of the zeroth order in ϵ as well as the third derivative in Eq. (9). In the limit $\epsilon \rightarrow 0$ at large κ for the caustics, the two simple stationary points $\xi^*(\epsilon)$ coincide and form one caustic point given by Eq. (9). To remove the in-determination, let us consider a small perturbation of the catastrophe integral $I(\epsilon, \kappa)$ [Eq. (8)] with changing ϵ through the phase function $\Phi(\xi, \epsilon)$ and the amplitude $A(\xi, \epsilon)$ near the caustic point $\epsilon = 0$. For *any small nonzero* ϵ we first study the expansion of the function $\Phi(\xi, \epsilon)$ over ϵ in a power series near the stationary point $\xi^*(\epsilon)$ for a small ϵ ,

$$\begin{aligned} \Phi(\xi, \epsilon) &= \Phi^* + \frac{1}{2} \Phi''(\xi^*) (\xi - \xi^*)^2 \\ &+ \frac{1}{6} \Phi'''(\xi^*) (\xi - \xi^*)^3 + \dots \end{aligned} \quad (10)$$

Similarly, for the amplitude expansion, one has

$$A(\xi, \epsilon) = A^* + A'(\xi^*) (\xi - \xi^*) + \dots \quad (11)$$

The asterisks in these two latter equations indicate that the derivatives with respect to ξ are taken at $\xi = \xi^*(\epsilon)$ for a small but finite ϵ , $\Phi^* = \Phi(\xi^*, \epsilon)$. Using a small perturbation of the action $\Phi(\xi, \epsilon)$ and amplitude $A(\xi, \epsilon)$ by ϵ variations, one finds the first derivative in Eq. (9) and the second derivative in Eq. (10) as small but nonzero quantities. For asymptotic values of $\kappa \rightarrow \infty$, one may truncate the series (10) for the phase $\Phi(\xi, \epsilon)$ in the exponent of the catastrophe integral $\mathcal{I}(\kappa, \epsilon)$ [Eq. (8)] and corresponding one (11) for its amplitude $A(\xi, \epsilon)$ at the third and zeroth orders, respectively, keeping however a *small nonzero* ϵ .

In the following, defining ξ as a dimensionless variable, one can simply take the second derivative of a phase Φ

in Eq. (10), divided by 2, as the parameter ϵ ,

$$\epsilon = \frac{1}{2} \Phi''(\xi^*) = \sigma |\epsilon|, \quad \sigma = \text{sign}(\epsilon) = \text{sign}(\Phi''(\xi^*)) . \quad (12)$$

By definition of the simplest caustic point of the first order [Eq. (9)], the third derivative of the phase Φ near the caustic point $\epsilon = 0$ is not zero at any small ϵ . Therefore, one can truncate the expansion of the phase integral (10) up to the third order as

$$\Phi = \Phi^* + \epsilon (\xi - \xi^*)^2 + a (\xi - \xi^*)^3, \quad (13)$$

where

$$a = \frac{1}{6} \Phi'''(\xi^*) . \quad (14)$$

Here, we assume that $A(\xi^*, \epsilon)$ has a *finite nonzero* limit at $\epsilon \rightarrow 0$. Therefore, it can be cut at zeroth order in $\xi - \xi^*$, namely, $A(\xi) \sim A^* = A(\xi^*, 0)$.

Following Refs. [20, 22], one can consider the *linear transformation* of the coordinate from ξ to z as

$$\xi - \xi^* = \Upsilon + \Lambda z, \quad (15)$$

where

$$\Upsilon = -\frac{\epsilon}{3a}, \quad \Lambda = \frac{1}{(3a\kappa)^{1/3}} . \quad (16)$$

Notice that both the coefficients of this linear transformation, $\Upsilon(\epsilon)$ and $\Lambda(\kappa)$, depend on different critical parameters ϵ and κ , respectively ($\Upsilon(0) = \Lambda(\infty) = 0$). Substituting Eq. (15) into Eq. (13), one can express the catastrophe integral (8) in an analytical form,

$$\begin{aligned} \mathcal{I}(\kappa, \epsilon) &= \pi \Lambda A^* \exp(i\kappa \Phi^* + \frac{2i\sigma}{3} w^{3/2}) \\ &\times [\text{Ai}(-w, \mathcal{Z}_-, \mathcal{Z}_+) + i \text{Gi}(-w, \mathcal{Z}_-, \mathcal{Z}_+)] . \end{aligned} \quad (17)$$

The generalized incomplete Airy and Gairy integrals are defined in a similar way as the standard ones but with the finite integration limits,

$$\left\{ \begin{array}{c} \text{Ai} \\ \text{Gi} \end{array} \right\} (-w, z_1, z_2) = \frac{1}{\pi} \int_{z_1}^{z_2} dz \left\{ \begin{array}{c} \cos \\ \sin \end{array} \right\} \left(-w z + \frac{z^3}{3} \right) . \quad (18)$$

The argument w of these functions and finite integration limits \mathcal{Z}_{\pm} in Eqs. (17) and (18) are given by

$$w = \frac{\kappa^{2/3} \epsilon^2}{(3a)^{4/3}} > 0, \quad (19)$$

and

$$\mathcal{Z}_{\pm} = \frac{\xi_{\pm} - \xi^*}{\Lambda} + \sigma \sqrt{w} . \quad (20)$$

As seen from a cubic form of the phase in the integrand exponent of Eq. (18), the caustic catastrophe can be considered as a crossing point of the two simple *close* stationary-point curves for any *small nonzero* ϵ ,

$$z_{\pm}^*(\epsilon) = \pm \sqrt{w(\epsilon)} . \quad (21)$$

¹ In general, the caustic point of the n th order ($n \geq 1$) is defined as the point where the derivatives up to the $(n+1)$ th order vanish but the $(n+2)$ th derivatives remain finite.

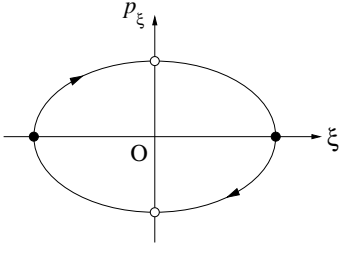


FIG. 1. Illustration of the phase-space flow around a PO at the origin in case of a regular trajectory on the torus. Open and solid dots represent caustic points ($\partial p_\xi / \partial \xi = 0$) and turning points ($\partial p_\xi / \partial \xi = \pm\infty$), respectively. The trajectory around the PO turns clockwise in the (ξ, p_ξ) plane and the curvature $\Phi'' \propto \partial p_\xi / \partial \xi$ changes its sign from positive to negative when the trajectory crosses the caustic point. At the crossings of the turning points, the curvature changes from $-\infty$ to $+\infty$.

They degenerate into one caustic point $z_\pm^*(\epsilon) \rightarrow 0$ (9) in the limit $\epsilon \rightarrow 0$ because of $w \rightarrow 0$ at any finite κ . The final result is a sum of the contributions of these stationary points. Note that, according to Eq. (19), the value of w is *large* for *any nonzero* ϵ when κ becomes large. Nevertheless, it becomes *small* for a *large fixed finite nonzero* κ when ϵ is *small*. However, we may consider the both cases by using the same formula (17) because the two parameters ϵ and κ appear in (19) through one parameter w for a finite constant a .

B. The Maslov theorem

For any small nonzero ϵ , one may find a value of κ for which w is so large that the two above-mentioned stationary points $z_\pm^*(\epsilon)$ can be treated *separately* in the SPM. At the same time, w can be enough small so that the stationary points $|z_\pm^*|$ are much smaller than the integration limits $|Z_\pm|$. In practice, it is enough to consider $Z_+ > 0$ and $Z_- < 0$, and we split the integration interval into two parts, i.e., from Z_- to 0 and from 0 to Z_+ , in order to separate the contributions of negative and positive stationary points, $-\sqrt{w}$ and \sqrt{w} . According to the phase-space flow around the PO (see Fig. 1), the curvature $\Phi'' \propto \partial p_\xi / \partial \xi$ (p_ξ denotes the momentum conjugate to ξ) will always change its sign from positive to negative at the caustic catastrophe point [18]. Let us consider such crossings with a catastrophe point. Outside of the catastrophe point, where $\epsilon > 0$ ($\sigma = 1$), the stationary point ξ^* corresponds to z_+^* and its contribution is given by the second integral over positive z . For this integral, one can extend the upper integration limit Z_+ to the *infinity*, like in the SSPM, because $Z_+ \propto \kappa^{1/3} \gg 1$ and $Z_+ \gg z_+^* = \sqrt{w} \propto \kappa^{1/3} \epsilon$ for a small finite ϵ , see Eq. (19). Within this approximation, one can use the

standard complete Airy and Gairy functions,

$$\begin{Bmatrix} \text{Ai} \\ \text{Gi} \end{Bmatrix}(-w) = \frac{1}{\pi} \int_0^\infty dz \begin{Bmatrix} \cos \\ \sin \end{Bmatrix} \left(-wz + \frac{z^3}{3} \right). \quad (22)$$

They correspond to the limits $z_1 = Z_- = 0$ and $z_2 = Z_+ = \infty$ in Eq. (18). Using the asymptotic form of the Airy and Gairy functions for $w \rightarrow \infty$

$$\begin{Bmatrix} \text{Ai} \\ \text{Gi} \end{Bmatrix}(-w) \rightarrow \frac{1}{\sqrt{\pi w^{1/4}}} \begin{Bmatrix} \sin \\ \cos \end{Bmatrix} \left(\frac{2}{3} w^{3/2} + \frac{\pi}{4} \right), \quad (23)$$

one can evaluate the contribution \mathcal{I}_+ of the positive stationary point to Eq. (17), asymptotically far from the caustic point (9). Then, one obtains the same result as we would get by the standard second-order expansion of the phase Φ (and zeroth order of the amplitude A) at a simple stationary point ξ^* ,

$$\begin{aligned} \mathcal{I}_+(\kappa, \epsilon) &\simeq \pi \Lambda A^* \exp \left(i\kappa \Phi^* + \frac{2i}{3} w^{3/2} \right) [\text{Ai}(-w) \\ &+ i\text{Gi}(-w)] \rightarrow \sqrt{\frac{2\pi}{\kappa |\Phi''(\xi^*)|}} A^* \exp \left(i\kappa \Phi^* + \frac{i\pi}{4} \right). \end{aligned} \quad (24)$$

On the other side of the crossing with the catastrophe point, $\epsilon < 0$ ($\sigma = -1$), the stationary point ξ^* corresponds to z_-^* . Therefore, one should consider the other part of the integral \mathcal{I}_- over the negative values of z . Obviously, considering in an analogous way with a change of the integration variable $z \rightarrow -z$, one obtains

$$\begin{aligned} \mathcal{I}_-(\kappa, \epsilon) &\simeq \pi \Lambda A^* \exp \left(i\kappa \Phi^* - \frac{2i}{3} w^{3/2} \right) [\text{Ai}(-w) \\ &- i\text{Gi}(-w)] \rightarrow \sqrt{\frac{2\pi}{\kappa |\Phi''(\xi^*)|}} A^* \exp \left(i\kappa \Phi^* - \frac{i\pi}{4} \right). \end{aligned} \quad (25)$$

Comparing the right-most expression in Eq. (25) with that in Eq. (24), one sees a shift of phase by $-\pi/2$. Thus, the famous Maslov theorem [21] on the shift of the phase Φ by $-\pi/2$ at each simple caustic point (9) of the CT (in particular, the PO) in the SSPM (i.e., the Maslov index is raised in one) has been proved by using the Fedoriuk catastrophe method [20].

For the case of a *turning point*, one has the conditions (9) with the only replace of zero by ∞ in the second derivative. In this case, Fedoriuk used a linear coordinate transformation from z to \tilde{z} , which has a form

$$z = \frac{\tilde{\Lambda}}{\epsilon} \tilde{z} + \tilde{\Upsilon}, \quad (26)$$

where $\tilde{\Lambda}$ and $\tilde{\Upsilon}$ are new constants which are not singular in ϵ ($\tilde{\Lambda}$ is independent of ϵ). This transformation reduces the turning-point singularity to the caustic-point one. Indeed, the divergent second derivative of the phase Φ over the variable z is transformed, in a new variable, to its zero value,

$$\frac{1}{2} \left(\frac{\partial^2 \Phi}{\partial^2 \tilde{z}} \right)^* = \frac{\tilde{\Lambda}^2}{\epsilon}; \quad (27)$$

see the second paper in Ref. [20]. Therefore, one obtains the same shift by $-\pi/2$ at each simplest turning point (per a sign change of one momentum component perpendicular to the boundary) along a CT. Finally, the next part of the Maslov theorem [21] concerning the Maslov index generated by such a turning point has been proved, too, within the same catastrophe theory of Fedoriuk [20].

IV. SYMMETRY-BREAKING AND BIFURCATIONS

Assuming a convergence of the expansion [Eq. (10)] to the second order, as shown in the previous Section, one can use the same approach within the simplest ISPM2 of second order² to investigate the symmetry-breaking and bifurcation problems in the POT. Therefore, one arrives at a sum over the separate contributions of different kinds of the isolated and degenerated orbits, as in the derivation of the Maslov theorem but within the *finite* integration limits. The latter is important because the bifurcation point is located at a boundary of the classically accessible region. This section is devoted to the extension of the FMCT to the bifurcation catastrophe problems.

In the presence of continuous symmetries, the stationary points form a family of POs which cover a $(\mathcal{K}+1)$ -dimensional submanifold \mathcal{Q}_{PO} of phase space, whereby \mathcal{K} is the classical degeneracy of the PO family. The integration over \mathcal{Q}_{PO} must be performed exactly. In any systems with continuous symmetries, it is an advantage to transform the phase space variables from the Cartesian to the corresponding action-angle variables (see, e.g., Ref. [8, 9]). Then, the action Φ_{CT} in Eq. (1) is independent of the angle variables conjugate to the conserving action variables, and the integrations over these cyclic angle variables are exactly carried out. For the integrable case, for instance, integrating over the remaining action variables and using the standard SPM, one obtains the so called Berry-Tabor trace formula [9]. Under the existence of additional symmetries like $\text{SU}(3)$ or $\text{O}(4)$, some of the integrations over the action variables can be also performed exactly because of a higher degeneracy. For partially integrable systems, the integrations over partial set of the cyclic variables also much simplify the ISPM derivations of the trace formula (1) near the bifurcations.

For solving the bifurcation problems, some of the SPM integrations have to be done in a more exact way. For definiteness, we shall consider first a *simple bifurcation* defined as a caustics of the first order [Eqs. (10) and (11)] where one has locally the increasing of degeneracy parameter \mathcal{K} in one unit. In the SPM, after performing

the exact integrations over a submanifold \mathcal{Q}_{PO} , one uses an expansion of the action phase Φ_{CT} in phase space variables $\xi = \{\mathbf{r}'', \mathbf{p}'\}_{\perp}$, perpendicular to \mathcal{Q}_{PO} in the integrand of Eq. (1) over ξ near the stationary point ξ^* ,

$$\Phi_{\text{CT}}(\xi) = \Phi_{\text{PO}} + \frac{1}{2}\Phi''_{\text{PO}}(\xi^*)(\xi - \xi^*)^2 + \frac{1}{6}\Phi'''_{\text{PO}}(\xi^*)(\xi - \xi^*)^3 + \dots, \quad (28)$$

where

$$\Phi_{\text{PO}} = \Phi_{\text{CT}}^* = \Phi_{\text{CT}}(\xi^*), \quad (29)$$

ξ^* is the stationary point, $\xi^* = \xi_{\text{PO}}$, and $\Phi_{\text{CT}}^* = \Phi_{\text{CT}}(\xi^*) = \Phi_{\text{PO}}$. To demonstrate the key point of our derivations of the trace formula, we focus on one of the phase-space variables in Eq. (1), denoted by ξ , which is associated with a catastrophe behavior. In the standard SPM, the above expansion is truncated at the 2nd order term, and the integration over the variable ξ is extended to $\pm\infty$. The integration can be performed analytically and yields a Fresnel integral; see, e.g., Refs. [4, 10].

However, one encounters a singularity in the SSPM which is related to zeros or infinities of $\Phi''_{\text{PO}}(\xi^*)$ while $\Phi'''_{\text{PO}}(\xi^*)$ remains finite in the simplest case under the consideration. This singularity occurs when a PO (isolated or degenerated) undergoes a *simple bifurcation* at the stationary point ξ^* under the variation of a parameter of the potential (e.g., energy, deformation, or the surface diffuseness). The SSPM approximation to the Fresnel (error) functions by the Gaussian integrals breaks down because one has a divergence.

Notice that the bifurcation problem is similar to the caustic singularity considered by Fedoriuk within the catastrophe theory (see Sec. III and Refs. [20, 22]). The FMCT is adopted, however, to the specific position of such a singularity at the end-point in the phase-space volume accessible for a classical motion (see Introduction, and also Ref. [13]).

In systems with continuous symmetries, the orbit at the end-point causes the bifurcation where it coincides with one of the rational tori which appears in the transition from the unphysical to the physical region. The contribution of this end-point orbit is derived using a local phase-space variable ξ along it, independently of the torus orbits. Near the bifurcation point, the contribution of these end-point orbits is mostly included into the new-born orbit term. Therefore, we should consider a kind of separation of the phase space occupied by the new-born and end-point orbits to evaluate their contributions to the trace integral near the bifurcation point. We shall call below the latter as an *end-point manifold*. By definition of the end-point manifold, its measure is zero at the bifurcation limit where the minimal ξ_- and maximal ξ_+ coincide with the stationary point ξ^* , i.e.,

$$\xi_- \rightarrow \xi_+ \rightarrow \xi^* \quad (\Phi''_{\text{PO}} \rightarrow 0). \quad (30)$$

Thus, although the contributions of POs participating in the bifurcation are considered separately, the parent

² We call the n th order ISPM as “ISPM n ”, in which we use the expansion of the phase integral Φ up to the n th order terms and the amplitude up to the $(n-2)$ th order near the stationary point. The simplest ISPM for $n = 2$ is called as ISPM2.

orbit contribution vanishes at the bifurcation point, and one has no danger of double counting. To describe the transition from the bifurcation point to the asymptotic region, one should properly define the end-point manifold. We need it to extract the additional contribution by the end-point orbit which is not covered by the term for the new-born orbit. The detailed treatment of such a transition, is still open and will be considered elsewhere in a forthcoming publication.

We are ready now to employ what we call the “improved stationary-phase method” (ISPM) [12–15] evaluating the trace integral for the semiclassical level density. Hereby, the integration over ξ in Eq. (1) is restricted to the *finite limits* defined by the classically allowed phase-space region through the energy-conserving delta function in the integrand of Eq. (1). The phase and the amplitude are expanded around the stationary point up to the second and zeroth order terms in $\xi - \xi^*$, respectively, and to higher order terms if necessary.

In the simplest version of the ISPM (ISPM2), the expansion of the phase is truncated at 2nd order, keeping the finite integration limits ξ_- and ξ_+ given by the accessible region of the classical motion in Eq. (1). It will lead to a factor like³

$$e^{i\Phi_{\text{PO}}/\hbar} \int_{\xi_-}^{\xi_+} \exp \left[\frac{i}{2\hbar} \Phi''_{\text{PO}} (\xi - \xi^*)^2 \right] d\xi \propto \frac{1}{\sqrt{\Phi''_{\text{PO}}}} e^{i\Phi_{\text{PO}}/\hbar} \text{erf}[\mathcal{Z}_-, \mathcal{Z}_+], \quad (31)$$

where $\text{erf}(z_1, z_2)$ is the generalized error function,

$$\text{erf}(z_1, z_2) = \frac{2}{\sqrt{\pi}} \int_{z_1}^{z_2} e^{-z^2} dz = \text{erf}(z_2) - \text{erf}(z_1), \quad (32)$$

with the complex arguments,

$$\mathcal{Z}_{\pm} = (\xi_{\pm} - \xi^*) \sqrt{-\frac{i}{2\hbar} \Phi''_{\text{PO}}}. \quad (33)$$

Note that the expression (31) has no divergence at the bifurcation point where $\Phi''_{\text{PO}}(\xi^*) = 0$, since the error function (32) also goes to zero as

$$\text{erf}(\mathcal{Z}_-, \mathcal{Z}_+) \propto \mathcal{Z}_+ - \mathcal{Z}_- \propto (\xi_+ - \xi_-) \sqrt{\Phi''_{\text{PO}}}. \quad (34)$$

Thus, the factor $\sqrt{\Phi''_{\text{PO}}}$ in the denominator of Eq. (31) is canceled with the same in the numerator. In addition, taking also into account Eq. (30) and discussions around it, one finds the zero contribution of the end-point term into the trace formula at the bifurcation point, which seems to be a consistent semiclassical picture.

This procedure is proved to be valid in the semiclassical limit, $\kappa \rightarrow \infty$, by the FMCT [20–22]. In this way, we can derive the separate PO contributions which are free of divergences, discontinuities, and double counting at any bifurcation point. The oscillating part of the level density can be approximated by the *semiclassical trace formula* (6). In Eq. (6), the sum runs all periodic orbits (isolated or degenerated) in the classical system. $S_{\text{PO}}(E)$ is the action integral along a PO. The amplitude $A_{\text{PO}}(E)$ (which, in general, is complex) is of the order of the phase space volume occupied by CTs. The factor given in Eq. (31) depends on the degeneracies and stability's of the POs, respectively; see Sec. III.

Notice that any additional exact integration in Eq. (1) with respect to a bifurcation (catastrophe) variable of the improved SPM can lead to an enhancement of the amplitude A_{PO} in the transition from the bifurcation point to the asymptotic region. This enhancement is of the order $1/\hbar^{1/2}$ as compared to the result of the standard SPM integration. In particular, for the new-born family with the extra degeneracy $\Delta\mathcal{K}$ higher than that of the parent PO, one has such enhancements of the order $1/\hbar^{\Delta\mathcal{K}/2}$ near the bifurcation.

The trace formula (6) thus relates the quantum oscillations in the level density to quantities which are purely determined by the classical system. Therefore, one can understand the shell effects in terms of classical pictures. The sum over POs in Eq. (6) is asymptotically correct to the leading order in $1/\hbar^{1/2}$, and it is hampered by convergence problems [2]. However, one is free from those problems by taking the *coarse-grained level density*,

$$\delta g_{\Gamma, \text{scl}}(E) = \sum_{\text{PO}} \delta g_{\text{PO}}^{\text{scl}}(E) \exp \left\{ - \left(\frac{\Gamma t_{\text{PO}}}{2\hbar} \right)^2 \right\}, \quad (35)$$

where Γ is an averaging width. The value of Γ is sufficiently smaller than the distance between the major shells near the Fermi surface, see Refs. [3–6, 10, 11]. $t_{\text{PO}} = \partial S_{\text{PO}}(E)/\partial E$ is the period of the particle motion along a PO taking into account its repetition number. We see that, depending on the smoothing width Γ , longer orbits are automatically suppressed in the above expressions, and the PO sum converges – which it usually does not [2] for non-integrable systems in the limit $\Gamma \rightarrow 0$. Thus, one can highlight the *major-shell structure* in the level density using a smoothing width which is much larger than the mean s.p. level spacing but smaller than the main shell spacing (the distance between major shells) near the Fermi surface. Alternatively, a finer shell structure can be considered by using essentially smaller smoothing widths, that is important for studying the symmetry breaking (bifurcation) phenomenon associated with longer POs.

It is the advantage of this approach that the major-shell effects in $\delta g(E)$ can be often explained semiclassically in terms of only a few shortest POs in the system. Examples will be given in Sec. V. However, if one wants to study a finer shell structure, specifically at large deformations, some longer orbits have to be included. Hereby,

³ For the case of several variables ξ for which we find zeros or infinities of eigenvalues of the matrix with second-order derivatives of $\Phi_{\text{PO}}(\xi)$ at $\xi = \xi^*$, we diagonalize this matrix and reduce the Fresnel-like integrals to products of error functions similar to Eq. (31).

bifurcations of POs play a crucial role, as it will be exemplified in Sec. V.

V. ISPM FOR THE SPHERICAL RPL POTENTIAL MODEL

Let us apply the general FMCT to the RPL potential as an analytically solvable example.

A. Scaling property

A realistic mean-field potential for nuclei and metallic clusters is given by the well-known WS potential,

$$V_{\text{WS}}(r) = -\frac{W_0}{1 + \exp \frac{r-R}{a}}, \quad (36)$$

where W_0 is the depth of the potential, R is the nuclear radius and a is the surface diffuseness. As suggested in Refs. [28, 31], this potential can be approximated by the RPL potential for a wide range of mass numbers as

$$V_{\text{WS}}(r) \approx -W_0 + \frac{W_0}{2}(r/R)^\alpha, \quad (37)$$

with an appropriate choice of the radial power parameter α . One finds a good agreement of the quantum spectra for the approximation (37) to the WS potential up to and around the Fermi energy E_F .

Eliminating the constant term in the right-hand side of (37), we define the RPL model Hamiltonian as

$$H = \frac{p^2}{2m} + V_0(r/R_0)^\alpha, \quad V_0 = \frac{\hbar^2}{mR_0^2}, \quad (38)$$

where m is the mass of a particle and R_0 is an arbitrary length parameter.

In the spherical RPL model (38), as well as in general spherical potential models, one has the diameter and circle POs which form the two-parametric ($\mathcal{K} = 2$) families. The diameter and circle POs have minimum and maximum values of the angular momentum $L = 0$ and L_C , respectively. They correspond to the end points of the energy surface $H(I_r, L) = E$ implicitly given by the relationship (see, e.g., Ref. [11]),

$$I_r = \frac{1}{\pi} \int_{r_{\min}}^{r_{\max}} p_r dr = I_r(E, L), \quad (39)$$

where p_r is the radial momentum,

$$p_r = \sqrt{p^2(E, L) - L^2/r^2}, \quad (40)$$

with p the particle momentum,

$$p(E, L) = \sqrt{2m(E - V(r))}. \quad (41)$$

The integration limits r_{\min} and r_{\max} in Eq. (39) are functions of the energy E and angular momentum L for a

given spherical potential. In the spherical RPL potential, they are defined by the two real roots of the transcendent equation for the variable r :

$$p_r(L, \alpha) \equiv \sqrt{2m(E - V_0(r/R_0)^\alpha) - L^2/r^2} = 0. \quad (42)$$

Another key quantity in the POT is the curvature of the energy surface (39),

$$K = \frac{\partial^2 I_r}{\partial L^2}. \quad (43)$$

Using the invariance of the equations of motion under the scale transformation

$$\begin{aligned} \mathbf{r} &\rightarrow s^{1/\alpha} \mathbf{r}, \quad \mathbf{p} \rightarrow s^{1/2} \mathbf{p}, \\ t &\rightarrow s^{1/2-1/\alpha} t \quad \text{for } E \rightarrow sE, \end{aligned} \quad (44)$$

one may factorize the action integral $S_{\text{PO}}(E)$ along the PO as

$$\begin{aligned} S_{\text{PO}}(E) &= \oint_{\text{PO}(E)} \mathbf{p} \cdot d\mathbf{r} \\ &= \left(\frac{E}{V_0}\right)^{\frac{1}{2} + \frac{1}{\alpha}} \oint_{\text{PO}(E=V_0)} \mathbf{p} \cdot d\mathbf{r} \equiv \hbar \mathcal{E} \tau_{\text{PO}}. \end{aligned} \quad (45)$$

In the last equation, we define the dimensionless variables \mathcal{E} and τ_{PO} , as classical characteristics of the particle motion,

$$\mathcal{E} = (E/V_0)^{\frac{1}{2} + \frac{1}{\alpha}} \quad (46)$$

and

$$\tau_{\text{PO}} = \frac{1}{\hbar} \oint_{\text{PO}(E=V_0)} \mathbf{p} \cdot d\mathbf{r}. \quad (47)$$

We call them the *scaled energy* and the *scaled period*, respectively. To realize the advantage of the scaling invariance under the transformation (44), it is helpful to use \mathcal{E} and τ_{PO} in place of the energy E and the period t_{PO} for the particle motion along a PO, respectively. In the HO limit ($\alpha \rightarrow 2$), \mathcal{E} and τ_{PO} are proportional to E and t_{PO} ; while in the cavity limit ($\alpha \rightarrow \infty$), they are proportional to the momentum p and the geometrical PO length \mathcal{L}_{PO} , respectively.

The PO condition (5) determines several PO families in the RPL potential, namely the polygon-like ($\mathcal{K} = 3$), the circular and diametric ($\mathcal{K} = 2$) POs. This condition for the integrable spherical Hamiltonian is identical to a resonance condition, which is expressed in the spherical variables r, θ, φ as

$$\omega_r/\omega_\theta = n_r/n_\theta, \quad \omega_\theta \equiv \omega_\varphi, \quad (48)$$

where ω_r , ω_θ and ω_φ are frequencies in the radial and angular motion. Fig. 2 shows these POs in the RPL potential (38) in the (τ, α) plane, where $\tau_{\text{PO}} = \tau(\alpha, L_{\text{PO}})$ is the scaled period for the PO specified by (n_r, n_θ) which satisfies the resonance condition (48). As shown in this

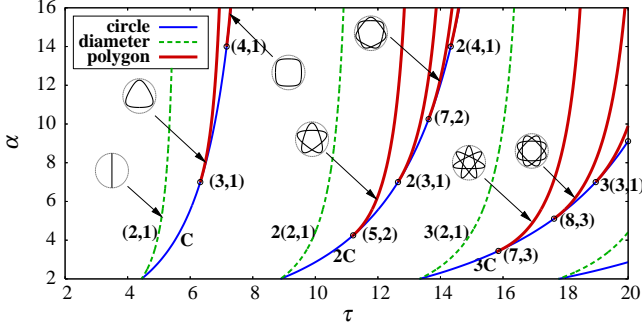


FIG. 2. The scaled periods τ_{PO} (horizontal axis) of some short periodic orbits PO plotted as functions of the power parameter α (vertical axis). Thin solid blue curves are circle orbits MC , dashed green curves are diameter orbits $M(2,1)$, and thick solid red curves are polygon-like orbits $M(n_r, n_\theta)$ ($n_r > 2n_\theta$) which bifurcate from the circle orbits MC at the bifurcation points indicated by open dots.

Figure, the polygon-like orbit $M(n_r, n_\theta)$ continues to exist after its emergence at the bifurcation point $\alpha = \alpha_{\text{bif}}$ from the parent circular orbit MC (M th repetition of the primitive circle orbit C). The exceptions are the diameter orbits $M(2,1)$ which exist for all values of α and form families with a higher degeneracy at the harmonic-oscillator (HO) symmetry-breaking point $\alpha = 2$.

B. Three-parametric PO families

For the contribution of the three-parametric ($\mathcal{K} = 3$) families into the density shell correction $\delta g(E)$ [Eq. (1)], one obtains [11]

$$\delta g_{\text{scl},P}(E) = \text{Re} \sum_{MP} A_{MP}(E) \times \exp \left[\frac{i}{\hbar} S_{MP}(E) - i \frac{\pi}{2} \mu_{MP} - i \phi_D \right]. \quad (49)$$

The sum is taken over families of the three-parametric ($\mathcal{K} = 3$) polygon-like orbits MP (“P” stands for “polygon-like”, and M accounts for the repetition number, $M = 1, 2, \dots$). In Eq. (49), $S_{MP}(E)$ is the action along the PO,

$$S_{MP}(E) = 2\pi M [n_r I_r(E, L^*) + n_\theta L^*], \quad (50)$$

where I_r is the radial action variable in the spherical phase-space coordinates [Eq. (39)]. The angular momentum L^* is given by the classical value for a particle motion along the P orbit, $L^* = L_P$, in an azimuthal plane. The numbers n_r and n_θ specify the orbit P with $n_r > 2n_\theta$. For the amplitude A_{MP} [Eq. (49)], within the ISPM2, one finds

$$A_{MP} = \frac{L_P T_P}{\pi \hbar^{5/2} \sqrt{M n_r K_P}} \text{erf}(\mathcal{Z}_{MP}^+, \mathcal{Z}_{MP}^-) e^{i\pi/4}, \quad (51)$$

where K_P represents the curvature (43), and $T_P = T_{n_r, n_\theta}$ is the period of the primitive ($M=1$) polygon-like orbit, $P(n_\theta, n_r)$. For a three-parametric family at the stationary point $L = L^*$ determined by the PO (stationary-phase) equation, one has

$$T_P = \frac{2\pi n_r}{\omega_r} = \frac{2\pi n_\theta}{\omega_\theta}. \quad (52)$$

The function $\text{erf}(\mathcal{Z}_{MP}^+, \mathcal{Z}_{MP}^-)$ in Eq. (51) is given by the generalized error function (32). Its complex arguments \mathcal{Z}_{MP}^\pm are expressed in terms of the curvature K_P ,

$$\mathcal{Z}_{MP}^- = \sqrt{-i\pi M n_r K_P / \hbar} (L_- - L_P), \quad \mathcal{Z}_{MP}^+ = \sqrt{-i\pi M n_r K_P / \hbar} (L_+ - L_P). \quad (53)$$

We used here the ISPM2 for the finite integration limits within the tori, i.e., between the minimal $L_- = 0$ and maximal $L_+ = L_C$ values of the angular-momentum integration variable for the $\mathcal{K} = 3$ family contribution. The phase factor μ_{MP} in Eq. (49) is the Maslov index (see Sec. III) as in the asymptotic Berry-Tabor trace formula. The amplitude (51) obtained for the formula (49) is regular at the bifurcation points where the stationary point is located at the end point $L = L^* = L_C$ of the action (L) part of a torus.

For the case of the power parameter α sufficiently far from the bifurcation points, one arrives at the SSPM limit of the trace formula (49) with the amplitude A_{MP} , identical to the Berry-Tabor trace formula [9],

$$A_{MP}^{(\text{SSP})} = \frac{2 L_P T_P}{\pi \hbar^{5/2} \sqrt{M n_r K_P}} e^{i\pi/4}. \quad (54)$$

According to Sec. III, the Maslov index μ_{MP} of Eq. (49) is determined by the number of turning and caustic points within the FMCT (see Refs. [13, 20–22]),

$$\mu_{MP} = 3 M n_r + 4 M n_\theta, \quad \phi_D = -\pi/2. \quad (55)$$

The total Maslov index $\mu_{MP}^{(\text{tot})}$ is defined as a sum of this asymptotic part (55) and the argument of the complex density amplitude (51) [10–14]. The total index $\mu_{MP}^{(\text{tot})}$ behaves as a smooth function of the energy E and the power parameter α through the bifurcation point.

C. Two-parametric circle families in the ISPM2

For contributions of the circular PO families to the trace formula (1), one obtains

$$\delta g_{\text{scl},C}(E) = \text{Re} \sum_M A_{MC} \times \exp \left[\frac{i}{\hbar} S_{MC}(E) - i \frac{\pi}{2} \mu_{MC} - i \phi_D \right]. \quad (56)$$

The sum is taken over the repetition number for the circle PO, $M = 1, 2, \dots$. $S_{MC}(E)$ is the action along the orbit

MC,

$$S_{MC}(E) = M \int_0^{2\pi} L d\theta = 2\pi M L_C, \quad (57)$$

where L_C is the angular momentum of the particle moving along the orbit C. For amplitudes of the MC-orbit contributions, one obtains

$$A_{MC}(E) = \frac{iL_C T_C}{\pi \hbar^2 \sqrt{F_{MC}}} \times \text{erf}\left(\mathcal{Z}_{pMC}^+\right) \text{erf}\left(\mathcal{Z}_{rMC}^-, \mathcal{Z}_{rMC}^+\right), \quad (58)$$

where $T_C = 2\pi/\omega_C$ is the period of a particle motion along the primitive ($M = 1$) orbit C. Here, ω_C is the azimuthal frequency,

$$\omega_C = \omega_\theta(L = L_C) = L_C/(m r_C^2), \quad (59)$$

r_C the radius of the C orbit, and L_C the angular momentum for a particle motion along the C PO [11, 28, 31, 37],

$$r_C = R_0 \left(\frac{2E}{(2+\alpha)V_0} \right)^{1/\alpha}, \quad L_C = p(r_C) r_C. \quad (60)$$

In Eq. (58), F_{MC} is the stability factor (the trace of the monodromy matrix),

$$F_{MC} = 4 \sin^2(\pi M \sqrt{\alpha+2}), \quad (61)$$

and $\mathcal{J}_{MC}^{(p)}$ is the Jacobian,

$$\mathcal{J}_{MC}^{(p)} = 2\pi(\alpha+2) M K_C r_C^2, \quad (62)$$

where K_C is the curvature for C orbits [37],

$$K_C = -\frac{(\alpha+1)(\alpha-2)}{12(\sqrt{\alpha+2})^3 L_C}. \quad (63)$$

The finite limits in the error functions of Eq. (58), \mathcal{Z}_{pMC}^\pm and \mathcal{Z}_{rMC}^\pm , are given by

$$\begin{aligned} \mathcal{Z}_{pMC}^- &= 0, \quad \mathcal{Z}_{pMC}^+ = L_C \sqrt{-\frac{i\pi}{\hbar}(\alpha+2) M K_C}, \\ \mathcal{Z}_{rMC}^- &= \left(\frac{r_{\min}}{r_C} - 1 \right) \sqrt{\frac{iF_{MC}}{4\pi(\alpha+2) \hbar M K_C}}, \\ \mathcal{Z}_{rMC}^+ &= \left(\frac{r_{\max}}{r_C} - 1 \right) \sqrt{\frac{iF_{MC}}{4\pi(\alpha+2) \hbar M K_C}}, \end{aligned} \quad (64)$$

where r_{\min} and r_{\max} are the radial turning points specified below. The interval between them covers the CT manifold including the stationary point r_C .

Asymptotically far from the bifurcations (also far from the symmetry breaking point $\alpha = 2$), the amplitude (58) approaches the SSPM limit:

$$A_{MC}(E) \rightarrow A_{MC}^{\text{SSP}}(E) = \frac{2L_C T_C}{\pi \hbar^2 \sqrt{F_{MC}}}. \quad (65)$$

In these SSPM derivations, the radial integration limits r_{\min} and r_{\max} turn into the asymptotic values,

$$r_{\min} = 0, \quad r_{\max} = R_0 \mathcal{E}^{2/(2+\alpha)}. \quad (66)$$

They are given by the two real solutions of Eq. (42) at $L = 0$. The upper limit r_{\max} was extended to ∞ in the derivation of Eq. (65) because the stationary point r_C is far away from the both integration boundaries r_{\min} and r_{\max} .

The Maslov index μ_{MC} in Eq. (56) is given by

$$\mu_{MC} = 2M, \quad \phi_D = \pi/2. \quad (67)$$

For the calculation of this asymptotic Maslov index μ_{MC} through the turning and caustic points [see the trace formula (56) with the ISPM2 (58) and the SSPM (65) amplitude], one can use the FMCT (Sec. III). The total Maslov index $\mu_{MC}^{(\text{tot})}$ can be introduced as above, see Refs. [10–14].

Taking the opposite limit $\alpha \rightarrow \alpha_{\text{bif}} = n_r^2/n_\theta^2 - 2$ to the bifurcations where $F_{MC} \rightarrow 0$, but far away from the HO limit $\alpha = 2$, one finds that the argument of the second error function in Eq. (58), coming from the radial-coordinate integration, tends to zero as $\propto \sqrt{|F_{MC}|}$ (64). Thus, as in a general case (Sec. IV), the singular stability factor $\sqrt{F_{MC}}$ of the denominator in Eq. (58) is exactly canceled by the same from the numerator. At the bifurcation $F_{MC} \rightarrow 0$, one obtains

$$A_{MC}^{\text{ISP}}(E) \rightarrow \frac{2L_C}{\hbar^{3/2} \omega_C \sqrt{i\pi(\alpha+2) M K_C r_C^2}} \times \text{erf}\left(\mathcal{Z}_{pMC}^{(+)}\right) (r_{\min} - r_{\max}). \quad (68)$$

Therefore, Eq. (58) gives the finite result through the bifurcation. Taking the shrink of the end-point manifold for the parent-orbit term, according to Eq. (30),

$$r_{\min} \rightarrow r_{\max} \rightarrow r_C, \quad (69)$$

the amplitude (58) vanishes at the bifurcation point [11], see Eq. (68). This is in line with general arguments for the bifurcation limit, see Sec. IV around Eq. (30).

As shown in Appendix A, following the FMCT (Section III) one can derive the ISPM3 expression for the oscillating level density. One may note that the parameter w given by Eq. (A3) can be considered as the dimensionless semiclassical measure of the distance from a bifurcation. Similarly, as for the caustic catastrophe points, in the case of the application of the FMCT (Sec. III) to the bifurcation of the circular orbits (see also Sec. V), one can use simply the ISPM2 (Sec. V C) as the simplest approximation near the bifurcation, i.e., $w \lesssim 1$. However, we have to work out properly the transition itself from the asymptotic SSPM radial-integration limits r_\pm to the same value r_C at the bifurcation within its close vicinity ($w \lesssim 1$) in the forthcoming publication.

D. Two-parametric diameter families

For the diameter-orbit ($\mathcal{K} = 2$) family contribution to the trace formula (1) for the RPL potential, the ISPM is needed only near the symmetry-breaking at $\alpha = 2$ of the harmonic oscillator limit [11]. As to our purpose, we simply use the SSPM approximation for the diameter families, valid at the values of the power parameter α far from the symmetry-breaking limit,

$$\delta g_{\text{scl D}}(E) = \text{Re} \sum_M A_{MD} \times \exp \left[\frac{i}{\hbar} S_{MD}(E) - \frac{i\pi}{2} \mu_{MD} - i\phi_D \right], \quad (70)$$

where

$$A_{MD} = \frac{1}{i\pi M K_D \omega_r \hbar^2}. \quad (71)$$

The frequency ω_r is expressed through the radial period,

$$T_r = \frac{2\pi}{\omega_r} = \int_0^{r_{\max}} \frac{2m dr}{p(r)} = \sqrt{\frac{2m\pi}{E}} \frac{r_{\max} \Gamma(1 + 1/\alpha)}{\Gamma(1/2 + 1/\alpha)}, \quad (72)$$

where $\Gamma(x)$ is the Γ function. In Eq. (71), K_D is the diameter curvature [37],

$$K_D = \frac{\Gamma(1 - 1/\alpha)}{\Gamma(1/2 - 1/\alpha) \mathcal{E} \sqrt{2\pi m R_0^2 V_0}}. \quad (73)$$

For the Maslov index [Eq. (70)], one obtains

$$\mu_{MD} = 2M, \quad \phi_D = -\pi/2. \quad (74)$$

E. TOTAL TRACE FORMULAS FOR THE SPHERICAL RPL POTENTIAL

The total ISPM trace formula for the RPL potential is the sum of the contribution of the $\mathcal{K} = 3$ polygon-like (P) families $\delta g_P(E)$ [Eqs. (49) with (51)], the $\mathcal{K} = 2$ circular (C) families $\delta g_C(E)$ [Eqs. (56) and (58) for the ISPM2 and Eqs. (A1) and (A2) for the ISPM3], and the $\mathcal{K} = 2$ diameter (D) families $\delta g_D(E)$ [Eqs. (70) and (71)],

$$\delta g_{\text{scl}}(E) = \delta g_{\text{scl,P}}(E) + \delta g_{\text{scl,C}}(E) + \delta g_{\text{scl,D}}(E). \quad (75)$$

This trace formula has the correct finite asymptotic limits to the SSPM: The Berry-Tabor result [Eqs. (49) and (54)] for the P orbits ($\mathcal{K} = 3$); and for C orbits ($\mathcal{K} = 2$) [Eqs. (56) and (65)]; see the same for D orbits, Eqs. (70) and (71)]. Transforming the variable from the ordinary energy E to the scaled energy \mathcal{E} (46), one obtains the trace formula for the scaled-energy level density,

$$\delta \mathcal{G}(\mathcal{E}) = \delta g(E) \frac{dE}{d\mathcal{E}} = \sum_{\text{PO}} \delta \mathcal{G}_{\text{PO}}(\mathcal{E}), \quad (76)$$

with

$$\delta \mathcal{G}_{\text{PO}}(\mathcal{E}) = \text{Re} [\mathcal{A}_{\text{PO}}(\mathcal{E}) \times \exp \left(i\mathcal{E}\tau_{\text{PO}} - \frac{i\pi}{2} \mu_{\text{PO}} - i\phi_D \right)]. \quad (77)$$

The Fourier transform of this scaled-energy level density, truncated by the Gaussian with the cut-off γ , is expressed as

$$F_\gamma(\tau) = \int \mathcal{G}(\mathcal{E}) e^{i\mathcal{E}\tau} e^{-(\mathcal{E}/\gamma)^2} d\mathcal{E} = \sum_{\text{PO}} \tilde{\mathcal{A}}_{\text{PO}}(\tau) e^{-\gamma^2(\tau - \tau_{\text{PO}})^2/4}. \quad (78)$$

This gives a function with successive peaks at the scaled periods of the classical POs $\tau = \tau_{\text{PO}}$ with the height $|\tilde{\mathcal{A}}_{\text{PO}}|$ which is proportional to the amplitude \mathcal{A}_{PO} of the contribution of the orbit PO to the semiclassical level density. Evaluating the same Fourier transform by the exact quantum level density, one has

$$F(\tau) = \int \left[\sum_i \delta(\mathcal{E} - \mathcal{E}_i) \right] e^{i\mathcal{E}\tau} e^{-(\mathcal{E}/\gamma)^2} d\mathcal{E} = \sum_i e^{i\mathcal{E}_i\tau} e^{-(\mathcal{E}_i/\gamma)^2}, \quad (79)$$

with

$$\mathcal{E}_i = (E_i/V_0)^{\frac{1}{2} + \frac{1}{\alpha}}. \quad (80)$$

Thus, one can extract the contribution of classical periodic orbits to the level density from the Fourier transform of the quantum level density. In what follows, we consider the classical-quantum correspondence using this Fourier transformation technique, in addition to the direct comparison of quantum and semiclassical level densities.

VI. COMPARISON WITH QUANTUM RESULTS

Figure 3 shows the Fourier transform of the quantum-mechanical level density $\mathcal{G}(\mathcal{E})$ for the RPL potential [see Eq. (79)]. At the HO limit $\alpha = 2$, all the classical orbits are periodic and form the 4-parametric family for a given energy. The Fourier transform exhibits the equidistant identical peaks at $\tau_n = \sqrt{2}\pi n$, corresponding to the n th repetitions of the primitive PO family. With increasing α , each peak is split into two peaks corresponding to the diameter (D) and circle (C) orbits, and the amplitudes of the oscillating level density for these orbits are decreased. However, one finds a growth of the peak at $\tau \sim 6.2$ corresponding to the C orbit around the bifurcation point $\alpha_{\text{bif}} = 7.0$. Note that, as approaching the bifurcation, the contribution of the C orbit is strongly enhanced until it forms a local family of POs with a higher degeneracy at the bifurcation point. From this

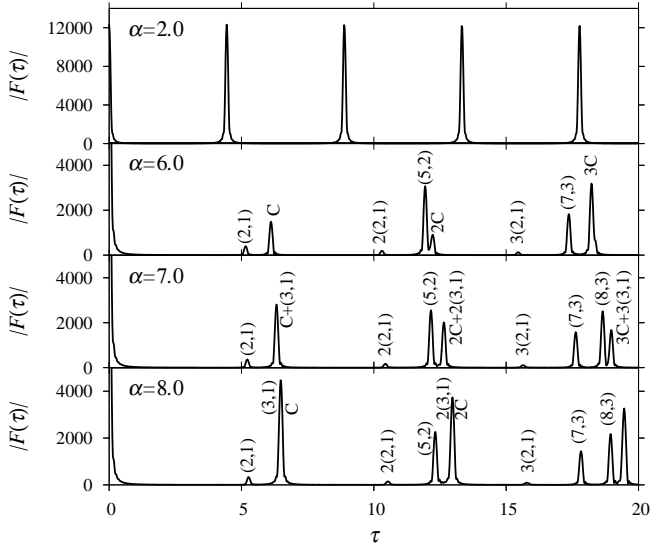


FIG. 3. Moduli of the Fourier transform $|F(\tau)|$ of the quantum scaled-energy level density [Eq. (79)] plotted for several values of α .

point a triangle-like P(3,1) families bifurcate. This family has the high degeneracy $\mathcal{K} = 3$. It remains important, also for larger $\alpha > \alpha_{\text{bif}}$. The above enhancement in the Fourier peaks $F(\tau)$ is directly associated with the oscillating ISPM level-density amplitude A_{PO} of the bifurcating PO family having a high degeneracy. This family makes a major term in the \hbar expansion in the comparison with the SSPM asymptotics (see Sec. IV and Ref. [11]). The Fourier peak at $\tau \sim 6.2$ in Fig. 3 shows the enhancement of the amplitude of the new-born P(3,1) family contribution including C(1,1) orbits as the end-points (see Introduction and Sec. IV).

As the significance of bifurcations is confirmed through the Fourier analysis [Eqs. (78) and (79)], let us now investigate the oscillating part of the scaled-energy level densities averaged with the Gaussian averaging parameter γ ,

$$\delta\mathcal{G}_\gamma(\mathcal{E}) = \int e^{-\left(\frac{\mathcal{E}-\mathcal{E}'}{\gamma}\right)^2} \delta\mathcal{G}(\mathcal{E}') d\mathcal{E}'. \quad (81)$$

The semiclassical shell-correction density, $\delta\mathcal{G}_{\gamma, \text{scl}}(\mathcal{E})$, is given by

$$\delta\mathcal{G}_{\gamma, \text{scl}}(\mathcal{E}) = \sum_{\text{PO}} \delta\mathcal{G}_{\text{PO}}(\mathcal{E}) \exp(-\tau_{\text{PO}}^2 \gamma^2 / 4). \quad (82)$$

[see Eq. (77) for $\delta\mathcal{G}_{\text{PO}}$]. For the quantum density, one has

$$\delta\mathcal{G}_{\gamma, \text{qm}} = \mathcal{G}_{\gamma, \text{qm}} - \tilde{\mathcal{G}}_{\text{qm}}, \quad (83)$$

where

$$\mathcal{G}_{\gamma, \text{qm}}(\mathcal{E}) = \sum_i e^{-\left(\frac{\mathcal{E}-\mathcal{E}_i}{\gamma}\right)^2}. \quad (84)$$

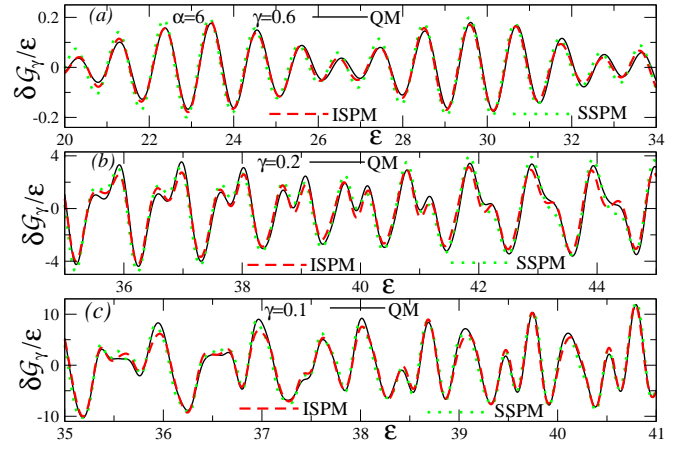


FIG. 4. Comparison of the quantum-mechanical (QM, black solid) and semiclassical [ISPM (red dashed) and SSPM (green dots)] shell-correction scaled-energy level density $\delta\mathcal{G}_\gamma(\mathcal{E})$ [(82) and (84)], divided by \mathcal{E} , as function of the scaled-energy \mathcal{E} for $\alpha = 6.0$ and averaging parameters $\gamma = 0.6$ [upper (a)], 0.2 [middle (b)], and 0.1 [bottom (c) panels].

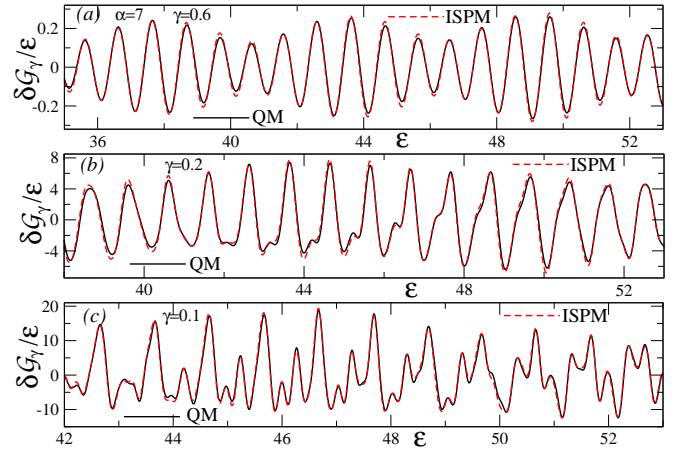


FIG. 5. Same QM and ISPM as in Fig. 4 but at $\alpha = 7.0$.

The smooth level density $\tilde{\mathcal{G}}_{\text{qm}}$ is calculated for the scaled spectrum \mathcal{E}_i . For these calculations we employed the standard Strutinsky averaging (over the scaled energy \mathcal{E}), finding a good plateau⁴ around the Gaussian averaging width $\tilde{\gamma} = 2 - 3$ and curvature-correction degree $\mathcal{M} = 6$.

Figs. 4–6 show a good agreement of the coarse-grained ($\gamma = 0.6$), and fine-resolved ($\gamma = 0.1 - 0.2$) semiclassical and quantum results for $\delta\mathcal{G}_\gamma(\mathcal{E})$ (divided by \mathcal{E}) as functions of the scaled energy \mathcal{E} at $\alpha = 6.0, 7.0$ and 8.0 . At $\alpha = 6$, as well as $\alpha = 2$ and 4 , the analytic expressions for all of the classical PO characteristics are available,

⁴ It may worth pointing out that the quality of the plateau in the SCM calculations of the level density is much better with using the scaled-energy variable \mathcal{E} rather than the energy E itself [37].

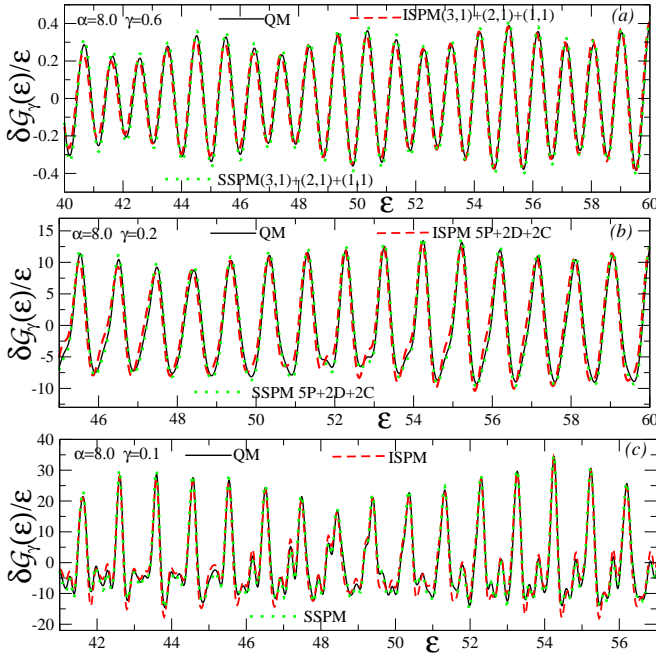


FIG. 6. Same as in Figs. 4 and 5 but for $\alpha = 8.0$; panel (a): major shell structure at $\gamma = 0.6$; panel (b): fine shell structure at $\gamma = 0.2$; panel (c): fine shell structure at $\gamma = 0.1$; the shortest POs and their numbers taken into account in the calculations are shown in the legends.

and can be used to check the precision of the numerical calculations [11, 37]. The values $\alpha = 6$ (Fig. 4) and 8 (Fig. 6) are taken as the examples which are sufficiently apart from the bifurcation point $\alpha = \alpha_{\text{bif}} = 7$ (Fig. 5). The ISPM results at these values of α show good convergences to the SSPM ones. The C and D POs with the shortest (scaled) periods τ are dominating the PO sum at a large averaging parameter $\gamma = 0.6$ (the coarse-grained or major-shell structure). Much more families with a relatively long period τ at $\gamma = 0.1 - 0.2$ (the fine-resolved shell structure) become significant in comparison with the quantum results (Ref. [11]).

Figure 5 shows the results for the bifurcation point $\alpha = 7$ where the triangle-like (3,1) PO family emerges from the parent C(1,1) family in a typical bifurcation scenario. One also finds good agreement of the ISPM with quantum results here. As the SSPM approximation fails at the bifurcation, it is not presented in Fig. 5. As discussed above, the SSPM at the bifurcation yields a sharp discontinuity of the P(3,1) amplitude, and a divergent behavior of the C(1,1); in contrast to the continuous ISPM components. Our results in Fig. 5 demonstrate that the ISPM successfully solves these catastrophe problems of the SSPM for all averaging parameters γ . In contrast to the results shown in Figs. 4 and 6, the coarse-grained ($\gamma = 0.6$) density oscillations at the bifurcation point $\alpha = 7$ (Fig. 5) do not contain any contributions from the C(1,1) end-point term but, instead, the P(3,1) term

becomes dominating.

Note that much more families with relatively long periods τ become necessary to account for the fine-resolved shell structures ($\gamma = 0.1 - 0.2$) [11]. For the exemplary bifurcation $\alpha = 7.0$, at smaller averaging parameters ($\gamma \lesssim 0.2$) the dominating orbits become the bifurcating newborn P(3,1) of the highest degeneracy $\mathcal{K} = 3$ along with the leading P(5,2), P(7,3), and P(8,3) POs which are born at smaller α (see Fig. 2). They include the parent C-orbit end-point manifolds. As also shown in the quantum Fourier transforms in Fig. 3, these POs yield larger contributions at the bifurcation values of α and even more enhanced on their right in a wide region of α .

VII. CONCLUSIONS

The Fedoriuk-Maslov catastrophe theory is extended to simple bifurcation problems in the POT. Within the extended FMCT, we overcome the divergence and discontinuity of semiclassical amplitudes of the standard stationary-phase method, in particular, in the Berry and Tabor formula near bifurcations. A fast convergence in the PO expansion of the averaged level density for a large Gaussian averaging parameter is shown too. This allows one often to express significant features of the shell structure in terms of a few short periodic orbits. We have formulated our ISPM trace formula for a simple bifurcation scenario so that the parent orbits at the *end points* have vanishing contributions at the bifurcation point, that allows to consider them everywhere separately from the term for a new-born family of the periodic orbits.

The extended FMCT is used for derivations of the trace formula in the case of the three-dimensional spherical RPL potential by employing the improved stationary phase method. We presented a class of the radial power-law potentials which, up to a constant provides a good approximation to the WS potential in the spatial region where the particles are bound. The RPL potential is capable of controlling surface diffuseness, and it contains the popular harmonic-oscillator and cavity potentials in the two limiting cases of the power parameter α . Its advantage is the scaling invariance of the classical equations of motion. This invariance makes the POT calculations and the Fourier analysis of the level density greatly easy. The contribution of the POs to the semiclassical level density and shell energies are expressed analytically (and even all the PO characteristics are given explicitly, e.g., for $\alpha = 6$) in terms of the simple special functions. The quantum Fourier spectra yield directly the amplitudes of the quantum level density at the periods (actions) of the corresponding classical POs.

We have derived the semiclassical trace formulas which are also valid in the bifurcation region, and examined them at the bifurcation catastrophe points and asymptotically far from them in the spherical RPL potential model. They are based on the SPM improved to account for the effect of the bifurcations by using the extended

FMCT. The ISPM overcomes the problems of singularities in the SSPM and provides the generic trace formula which relates the oscillating component of the level density for a quantum system to a sum over POs of the corresponding classical system. We showed a good convergence of this improved trace formula to the simplest ISPM based on the second-order expansion of the classical action at several characteristic values of the power parameter α including the bifurcations and, asymptotically far from them (see Appendix).

We obtained good agreement between the ISPM semiclassical and quantum results for the level density shell corrections at different values of the power parameter α , both at the bifurcations and far from them. At sufficiently far from the bifurcation of the leading short POs with a maximal degeneracy, one finds also a good convergence of the ISPM trace formulas to the SSPM approximation. We emphasize a significant influence of the bifurcations of short POs on the main characteristics of oscillating components of the single-particle level density for a fermionic quantum system. They appear in the significant fluctuations of the energy spectrum (visualized by its Fourier transform), namely, the shell structure.

In line with the general arguments of the extended FMCT (Sec. IV), the stationary points forming the circular-orbit families are located at the end point of the classically accessible region, and they coincide with the newborn family of the polygon-like orbits at the bifurcation. Taking into account the shrink of the end-point manifold in the bifurcation limit, the parent C-family contribution is transformed into the newborn P-family term which presents now their common result. Thus, one has the separate contributions of the parent C and new-born P orbits through the bifurcation scenario, but with no concern about a double counting.

In our future work we intend first to study in details the transition of the ISPM trace formula from the bifurcation points to its asymptotical SSPM region. This will enable us to understand more properly the shape dynamics of the finite fermion systems. In particular, the improved stationary phase method can be applied to describe the deformed shell structures where bifurcations play the essential role in formations of the superdeformed minima along a potential energy valley [10, 11]. One of the remarkable tasks might be to clarify, in terms of the summetry-breaking (restoration) and bifurcation phenomena, the reasons of the exotic deformations such as the octupole and tetrahedral ones within the suggested ISPM. In this way, it would be worth extending our present local bifurcation FMCT to describe, e.g., a bridge (non-local) bifurcation phenomenon found in a more realistic mean field in the fermionic systems, see also Refs. [31, 35, 36, 38].

Our semiclassical analysis may, therefore, lead to a deeper understanding of the shell effects in the finite fermionic systems such as atomic nuclei, metallic clusters, the trapped fermionic atoms, and the semiconductor quantum dots [4, 29, 30, 39–41]. Their level den-

sities, conductance and magnetic susceptibilities are significantly modified by shell effects. As a first step towards the collective dynamics, the oscillating parts of the nuclear moment of inertia will be studied semiclassically in terms of POs taking into account the bifurcations [42–45].

ACKNOWLEDGMENTS

Authors gratefully acknowledge M. Brack and K. Matsuyanagi for fruitful collaborations and many useful discussions. One of us (A.G.M.) is also very grateful for a kind hospitality during his working visits of Physical Department of the Nagoya Institute of Technology, also the Japanese Society of Promotion of Sciences for financial support, Grant No. S-14130.

Appendix A: The ISPM3 approximation

Following FMCT (Section III), one can derive the improved (ISPM3) contribution of the C orbits by taking into account the third order terms of the action expansion [see Eq. (10)] in the integration over the catastrophe variable r . Within the ISPM3, one obtains

$$\delta g_{\text{scl,C}}^{(3)}(E) = \text{Re} \sum_M A_{MC}^{(3)} \times \exp \left[\frac{i}{\hbar} S_{MC}(E) - \frac{i\pi}{2} \mu_{MC} + \frac{2i}{3} w^{3/2} - i\phi_{\mathcal{D}} \right]. \quad (\text{A1})$$

The ISPM3 amplitudes $A_{MC}^{(3)}$ are given by

$$A_{MC}^{(3)} = \frac{2\Lambda \sqrt{L_C}}{\hbar^{5/2} \omega_C} \frac{\text{erf} \left(\mathcal{Z}_{p,MC}^+ \right)}{\sqrt{2\pi i (\alpha + 2) M K_C}} \times \left[\text{Ai} \left(-w, \mathcal{Z}_{MC}^{(-,3)}, \mathcal{Z}_{MC}^{(+,3)} \right) + i \text{Gi} \left(-w, \mathcal{Z}_{MC}^{(-,3)}, \mathcal{Z}_{MC}^{(+,3)} \right) \right]. \quad (\text{A2})$$

where

$$w = w_{MC} = \left[\frac{\kappa^{1/3} F_{MC}}{4\pi(\alpha + 2) M K_C L_C (3a)^{2/3}} \right]^2, \quad (\text{A3})$$

with

$$a = \frac{r_C^3}{6L_C} \Phi_{\text{CT}}'''(r_C), \quad \text{and} \quad \kappa = \frac{L_C}{\hbar}. \quad (\text{A4})$$

The parameter ϵ of Eq. (8) [Eq. (12)] used in deriving the above expressions is proportional to the stability factor F_{MC} [Eq. (61)],

$$\epsilon = \frac{F_{MC}}{4\pi(\alpha + 2) M K_C L_C}. \quad (\text{A5})$$

The incomplete Ai (Gi) integrals in Eq. (A2) are defined by Eq. (18). The integration limits of these functions are the same as those given by Eq. (20),

$$Z_{MC}^{(\pm,3)} = \frac{r_{\pm} - r_C}{r_C \Lambda} + \sigma \sqrt{w_{MC}}, \quad \sigma = \text{sign}(\epsilon), \quad (\text{A6})$$

where r_{\pm} are the upper ($r_+ > r_C$) and the lower ($r_- < r_C$) limits for the radial integration. These integration limits are defined in Eq. (66). In the bifurcation limit $\alpha \rightarrow \alpha_{\text{bif}}$, both terms in the square brackets of Eq. (A2) [see also Eq. (A6)] go to zero by the same reason as in the ISPM2 case. The incomplete Ai and Gi functions of the integrand [Eq. (18)] have no singularities in the bifurcation limit $w \rightarrow 0$. In addition, the radial integration limits, r_{\min} and r_{\max} , approach the stationary point $r^* = r_C$, which is the C-orbit radius [Eq. (69)]. This ensures the disappearance of the end-point manifold in this limit, and therefore, in line with the general arguments of Sec. IV (see also Sec. VC), one finds the zero contribution of the circular orbits term exactly at this bifurcation. In place, the contribution of the circular orbit is included altogether in the new-born P orbit term.

In the opposite limit, sufficiently far from the bifurcation points, where the stability factor $F_{MC}(\alpha)$ takes a finite nonzero value, the second term in Eq. (A6) changes with increasing ϵ much faster ($\propto \kappa^{1/3}\epsilon$) than the first component ($\propto \kappa^{1/3}$). Thus, one has $|Z_{MC}^{(\pm,3)}| \gg |z_{MC}^{*,\pm}|$

in this limit. The ISPM3 expression [Eq. (A1) with Eq. (A2)] for the oscillating level density suggests that the parameter w ($w \propto F_{MC}^2 \propto \epsilon^2$) can be considered as the dimensionless measure of the distance from the bifurcation, see Eqs. (A3) and (A5). For a large distance from the bifurcation, $w \gg 1$ [Eq. (A3)], one can extend the radial integration limits as $r_- = 0$, $r_+ \rightarrow \infty$. In this limit, the incomplete Airy and Gairy functions (18) can be approximated by the complete ones (22). Since the argument w of these standard functions [Eq. (A3)] at a finite stability factor $F_{MC}(\alpha)$ becomes large in the semiclassical limit, $\kappa \gg 1$, one can use their asymptotic expressions (23). Thus, we arrive at the same SSPM result [Eqs. (56) and (65)] for the C family contributions as obtained from the ISPM2 C-trace formula [see Eq. (A2) for its amplitude].

For the simplest catastrophe problem, the ISPM3 might become important when the PO is distant from the bifurcation points to some extent but not asymptotically far from them. It is also necessary for the higher order catastrophe problem, which are not found in the RPL model discussed in this paper. The definition of the end-point manifold might be also affected by the consideration of the higher expansion term. This is also a future problem to be solved in order to describe the transition from a bifurcation vicinity to the asymptotic region.

-
- [1] M. C. Gutzwiller, J. Math. Phys. **12**, 343 (1971).
 - [2] M. C. Gutzwiller, *Chaos in Classical and Quantum Mechanics* (Springer-Verlag, N.Y., 1990).
 - [3] R. B. Balian and C. Bloch, Ann. Phys. (N.Y.) **69**, 76 (1972).
 - [4] M. Brack and R. K. Bhaduri, *Semiclassical Physics* (revised edition: Westview Press, Boulder, USA, 2003).
 - [5] V. M. Strutinsky, Nucleonika **20**, 679 (1975); V. M. Strutinsky and A. G. Magner, Fiz. Elem. Chast. At. Nucl. **7**, 356 (1976) [Sov. J. Part. Nucl. **7**, 138 (1976)].
 - [6] V. M. Strutinsky, A. G. Magner, S. R. Ofengenden, and T. Døssing, Z. Phys. A **283**, 269 (1977).
 - [7] A. G. Magner, Yad. Fiz. **28**, 1477 (1978) [Sov. J. Nucl. Phys. **28**, 759 (1978)].
 - [8] S. C. Creagh, J. M. Robbins, and R. G. Littlejohn, Phys. Rev. A **42**, 1907 (1990); S. C. Creagh, R. G. Littlejohn, Phys. Rev. A **44**, 836 (1991); J. Phys. A **25**, 1643 (1992).
 - [9] M. V. Berry and M. Tabor, Proc. R. Soc. Lond. A **349**, 101 (1976); **356**, 375 (1977).
 - [10] A. G. Magner, I. S. Yatsyshyn, K. Arita, and M. Brack, Yad. Fiz. **74**, 1 (2011) [Phys. Atom. Nucl. **74**, 1445 (2011)].
 - [11] A. G. Magner, M. V. Koliesnik, K. Arita, Phys. Atom. Nucl. , **79**, 1067 (2016).
 - [12] A. G. Magner, K. Arita, S. N. Fedotkin, and K. Matsuyanagi, Prog. Theor. Phys. **108**, 853 (2002).
 - [13] A. G. Magner, K. Arita, and S. N. Fedotkin, Prog. Theor. Phys. **115**, 523 (2006).
 - [14] A. G. Magner, S. N. Fedotkin, K. Arita, T. Misu K. Matsuyanagi, T. Schachner, and M. Brack, Prog. Theor. Phys. **102**, 551 (1999).
 - [15] A. G. Magner, S. N. Fedotkin, K. Arita, K. Matsuyanagi, and M. Brack, Phys. Rev. E **63**, 065201(R) (2001).
 - [16] M. V. Koliesnik, Ya. D. Krivenko-Emetov, A. G. Magner, K. Arita, and M. Brack, Phys. Scr. **90**, 114011 (2015).
 - [17] A. M. Ozorio de Almeida and J. H. Hannay, J. Phys. A **20** 5837 (1987).
 - [18] A. M. Ozorio de Almeida: *Hamiltonian Systems: Chaos and Quantization* (Cambridge University Press, Cambridge, 1988).
 - [19] K. R. Meyer, Transactions of the American Mathematical Society, **149**, 95 (1970).
 - [20] M. V. Fedoriuk, Sov. J. Com. Math. Math. Phys. **2**, 145 (1962); **4**, 671 (1964).
 - [21] M. P. Maslov, Theor. Math. Phys. **2**, 30 (1970).
 - [22] M. V. Fedoriuk, *The saddle-point method (Metod perevala*, Nauka, Moscow, 1977).
 - [23] D. Ullmo, M. Grinberg, and S. Tomsovic, Phys. Rev. E **54**, 136 (1996).
 - [24] M. Sieber, J. Phys. A **30**, 4563 (1997).
 - [25] H. Schomerus and M. Sieber, J. Phys. A **30** 4537 (1997); M. Sieber and H. Schomerus, J. Phys. A **31**, 165 (1998).
 - [26] H. Schomerus, J. Phys. A: Math. Gen. **31**, 4167 (1998).
 - [27] Ch. Amann and M. Brack, J. Phys. A: Math. Gen. **35** 6009 (2002).
 - [28] K. Arita, Int. J. Mod. Phys. E **13** 191 (2004).
 - [29] M. Brack, M. Ögren, Y. Yu, and S. M. Reimann, J. Phys. A **38**, 9941 (2005).

- [30] K. Arita and M. Brack, J. Phys. A **41**, 385207 (2008).
- [31] K. Arita, Phys. Rev. C **86**, 034317 (2012).
- [32] J. Moller-Anderson and M. Ögren, Rep. Math. Phys. **75**, 359 (2015).
- [33] V. M. Strutinsky, Nucl. Phys. A, **95**, 420 (1967); **122**, 1 (1968).
- [34] M. Brack, J. Damgaard, A. S. Jensen *et al.*, Rev. Mod. Phys. **44**, 320 (1972).
- [35] K. Arita, Physica Scripta, **91**, 063002 (2016).
- [36] K. Arita, Physica Scripta, **92**, 074005 (2017).
- [37] A. G. Magner, A. A. Vlasenko, K. Arita, Phys. Rev. E **87**, 062916 (2013).
- [38] K. Arita and Y. Mukumoto, Phys. Rev. C **89**, 054308 (2014).
- [39] S. Reimann, M. Brack, A. G. Magner, *et al.*, Phys. Rev. A **53**, 39 (1996).
- [40] M. Brack, J. Blaschke, S. C. Creagh, *et al.*, Z. Phys. D **40**, 276 (1997).
- [41] S. Frauendorf, V. M. Kolomietz, A. G. Magner and A. I. Sanzhur, Phys. Rev. B **58**, 5622 (1998).
- [42] A.G. Magner, A.S. Sitdikov, A.A. Khamzin, and J. Bartel, Phys. Rev. C **81**, 064302 (2010).
- [43] A. G. Magner, D. V. Gorpichenko, and J. Bartel, Phys. Atom. Nucl. **77**, 1229 (2014).
- [44] D. V. Gorpichenko, A. G. Magner, J. Bartel, and J. P. Blocki, Phys. Rev. C **93**, 024304 (2016).
- [45] A.G. Magner, D.V. Gorpichenko, and J. Bartel, Phys. At. Nucl. , **80**, 122 (2017).